

Supplemental Methods

Postmortem AD Brain Tissues

Frozen tissues of temporal cortex from neuropathologically confirmed AD patients without TDP-43 proteinopathies, primary argyrophilic grain disease, and α -synucleinopathies were provided by the Mayo Clinic brain bank at Jacksonville. Braak neurofibrillary tangle stage, Thal amyloid phase, and CAA score were evaluated by Thioflavin S fluorescent immunohistochemistry. CAA scores in the inferior parietal cortex, middle frontal cortex, motor cortex, superior temporal cortex and visual cortex in each subject were averaged (Supplemental Table 1). The cohort and ELISA measurements of A β overlapped with that of our previous study (14).

Animals

By breeding *Lrp1* floxed mice (*Lrp1^{fllox/fllox}*) with α -calcium-calmodulin-dependent kinase II (*α CaMKII*)-driven *Cre* recombinase mice (*α CaMKII-*Cre*^{+/-}*), *nLrp1^{-/-}* mice (*Lrp1^{fllox/fllox}*, *α CaMKII-*Cre*^{+/-}*) were generated. The *nLrp1^{-/-}* mice carrying APP/PS1 background (*APP/PS1^{+/-}*, *Lrp1^{fllox/fllox}*, *α CaMKII-*Cre*^{+/-}*) (15-17) were further crossed with APOE3-TR or APOE4-TR (18). Both male and female littermates of the following 4 groups of mice were used in this study: 1) APP/PS1; APOE3 control (*APP/PS1^{+/-}*, *APOE3^{+/+}*, *Lrp1^{fllox/fllox}*, *α CaMKII-*Cre*^{+/-}*); 2) APP/PS1; APOE3; *nLrp1^{-/-}* (*APP/PS1^{+/-}*, *APOE3^{+/+}*, *Lrp1^{fllox/fllox}*, *α CaMKII-*Cre*^{+/-}*); 3) APP/PS1; APOE4 control (*APP/PS1^{+/-}*, *APOE4^{+/+}*, *Lrp1^{fllox/fllox}*, *α CaMKII-*Cre*^{+/-}*); and 4) APP/PS1; APOE4; *nLrp1^{-/-}*

(*APP/PS1*^{+/-}, *APOE4*^{+/+}, *Lrp1*^{fllox/fllox}, *αCaMKII-Cre*^{+/-}) mice. Following transcardial perfusion with phosphate-buffered saline (PBS), mouse brains were dissected and kept at -80°C until further analysis. For histologic analysis, brain tissues from some mice were subsequently fixed in 10% formalin.

Sample preparation

The three-step extraction method using TBS, TBS-X and GDN-HCl were utilized to prepare lysates from postmortem AD brain and mouse brain samples (14, 20). Using a Polytron homogenizer (KINEMATICA), frozen brain tissues (100–200 mg) were first homogenized in 10-15 volumes (w/v) of ice-cold TBS containing protease inhibitor cocktail (Roche Diagnostics). Samples were then centrifuged at 100,000 x g for 60 min at 4°C, and the supernatant was used to measure components in the TBS fraction. The remaining pellet was next re-homogenized in TBS-X containing protease inhibitor cocktail, followed by incubation for 1 h at 4°C with mild agitation. After centrifuged as described above, the obtained supernatant was used to measure components in TBS-X fraction. Finally, the remaining pellet was re-homogenized in 5 M GDN-HCl (pH 7.6). The samples were centrifuged as above after incubation of the samples for 12–16 h at 22°C with mild agitation, and the supernatant (GDN-HCl fraction) was subjected to the dilution with nine volumes of TBS. All lysates in each fraction were aliquoted and stored at -80°C until used for analyses.

ELISAs

To measure concentrations of A β 40, A β 42, apoE, CTF β , LRP1, LDLR, GFAP, CD11b, PSD95 and synaptophysin in specific fractions from brain lysates, ELISAs using horseradish peroxidase (HRP)-linked streptavidin (Vector Laboratories) and/or 3,3',5,5'-tetramethylbenzidine substrate (Sigma) were performed as previously described (Supplemental Table 2) (12-14, 27). The signals were colorimetrically quantified using a Synergy HT plate reader (BioTek), and ELISA measurements were normalized to the total protein concentrations determined by BCA assay (Thermo Fisher).

Immunohistochemical analyses

Paraffin sections were prepared from mouse brains, and immunostained using anti-human A β 1-16 (33.1.1) (produced in house) (16, 22), anti-GFAP (BioGenex, Cat#PU020), and anti-ionized calcium-binding adaptor molecule 1 (Iba-1) (Wako, Cat#016-20001) antibodies (22), followed by visualization through the Dako Envision Plus visualization system (Dako, Carpinteria, CA). The images were captured using a Scanscope XT image scanner (Aperio Technologies, Vista, CA). For A β plaque burden assessment, A β deposition in the entire brain section, hippocampus and cortex immediately dorsal to the hippocampus was algorithmically measured by calculating the immunoreactivity utilizing the Positive Pixel Count program in the ImageScope software (Aperio Technologies). For CAA quantification, the burden of amyloid deposition in leptomeningeal arteries (13-15 arteries/mouse) was quantified by the Positive Pixel Count program (Aperio

Technologies). Double-immunofluorescent staining was performed using a rabbit polyclonal anti-LRP1 antibody (produced in house) (16), and a mouse monoclonal anti-NeuN antibody (Millipore, Cat#MAB377). Subsequently, the brain sections were incubated with Alexa488-conjugated anti-rabbit IgG (Invitrogen) and Alexa568-conjugated anti-mouse IgG (Invitrogen). Nuclei were visualized using mounting medium with DAPI (Vector Laboratories). Confocal laser-scanning fluorescence microscopy was used to obtain images (model LSM 510 invert; Carl Zeiss, Jena, Germany).

In vivo microdialysis

In vivo microdialysis was performed essentially as described (9, 22). Briefly, microdialysis probes were inserted into the hippocampus of mice at least 6 hours before experiments, and the ISF levels of A β 40 were measured over 7.5 hours using a constant flow of microdialysis perfusion buffer containing 0.15% bovine serum albumin (Sigma) in artificial cerebral spinal fluid (CSF) at the rate of 1.0 μ l/min. The basal levels were defined as the mean concentration of A β in the collected microdialysis perfusion buffer during this period. To assess A β clearance, a γ -secretase inhibitor compound E (AsisChem, Waltham, MA, USA) was directly injected into the hippocampus through the microdialysis probe into each mouse at the concentration of 200 nM. Microdialysis perfusion buffer was collected every hour for 5 hours following treatment with compound E. A β 40 levels were quantified by ELISA using mHJ2 (mouse-anti-A β 35-40) capture antibody and

biotinylated mHJ5.1 (mouse-anti-A β 13-28) detector antibody (provided by Dr. David M. Holtzman).

Statistics

For human data, associations of *APOE* genotypes with A β 40, A β 42, LRP1 or LDLR were addressed through multivariate regression models with adjustment to age, sex, Braak stage, Thal and averaged CAA scores. Interaction between *APOE* genotypes and LRP1 or LDLR levels with A β levels were also studied using multivariate logistic regression by adjusting for age, sex, Braak stage, Thal and averaged CAA scores. For animal experiments, statistical significance was determined by Tukey's post-hoc analysis after two-way Analysis of Variance (ANOVA) with adjustment for sex. Associations between A β and apoE levels were assessed through a linear regression model. In ISF A β 40 clearance assessment, statistical significance was determined by two-tailed student's t test. In each analysis, variables which were over 3-fold of SD from the mean value in the entire cohort were excluded as outliers. All statistical analyses were performed with JMP statistical software, and $p < .05$ was considered significant.

References

27. Shinohara M, Kanekiyo T, Yang L, Linthicum D, Shinohara M, Fu Y, Price L, Frisch-Daiello JL, Han X, Fryer JD, et al. APOE2 eases cognitive decline during Aging: Clinical and preclinical evaluations. *Ann Neurol*. 2016.

Supplemental table 1.**Subject characteristics of postmortem AD cohort**

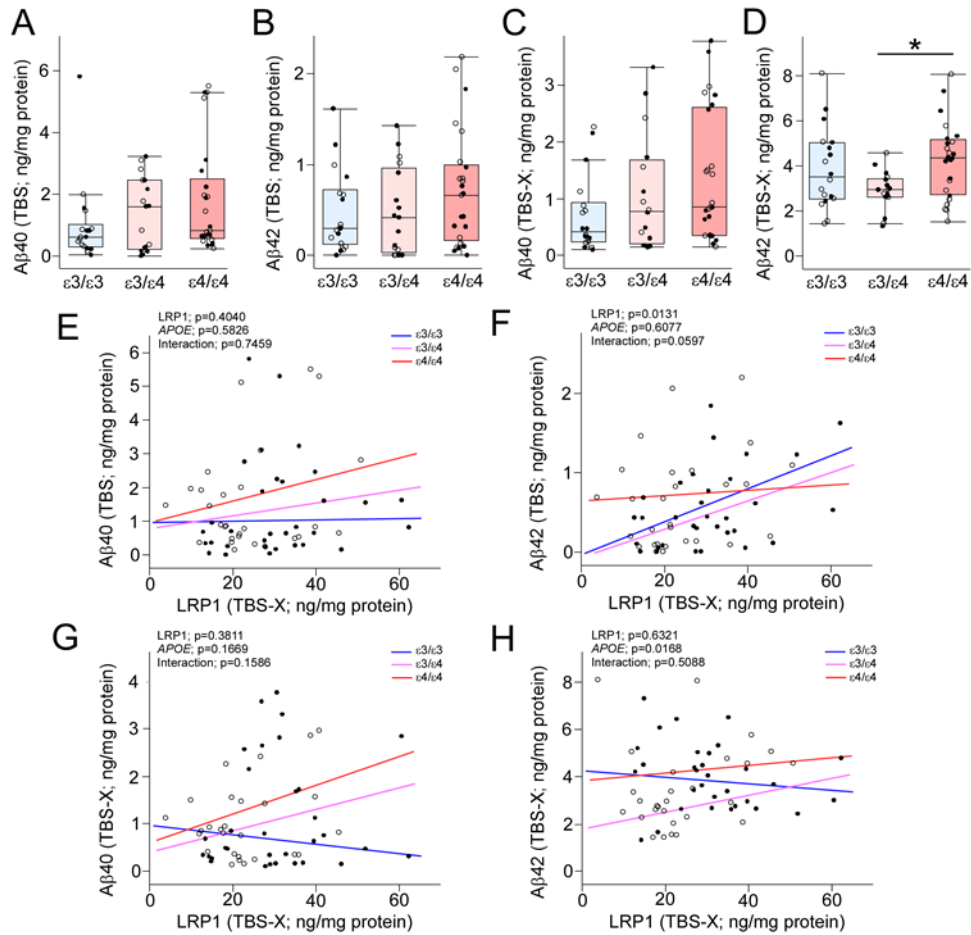
	<i>APOE</i> ε3/ε3 (N=18)	<i>APOE</i> ε3/ε4 (N=17)	<i>APOE</i> ε4/ε4 (N=25)
Age; year	79.5 (77-86)	79 (68-93)	83 (71-94)
Sex; male	8 (44.4)	11 (64.7)	13 (52.0)
Braak Stage			
<5	1 (5.6)	1 (5.9)	1 (2.0)
5-6	17 (94.4)	16 (94.1)	24 (96.0)
Thal Stage			
3	0 (0)	0 (0)	4 (16.0)
4	1 (5.6)	1 (5.9)	5 (20.0)
5	17 (94.4)	16 (94.1)	16 (64.0)
CAA score	2.4 (2.0-3.4)	2.6 (2.0-3.0)	2.6 (2.0-3.8)

Median and range shown for age and CAA score;

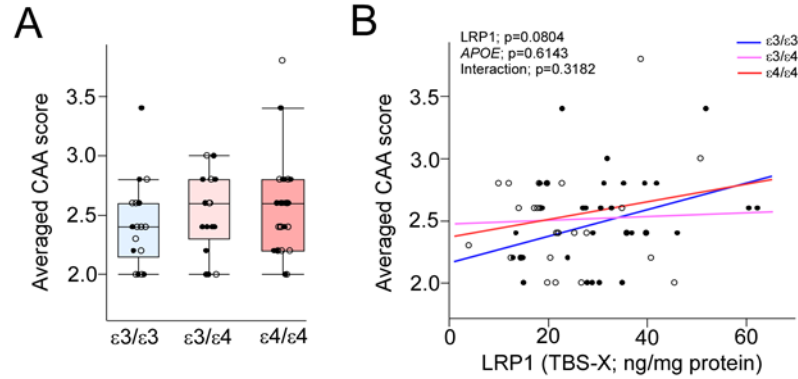
Number (%) shown for sex, Braak stage and Thal stage.

Supplemental table 2. Antibody list for ELISA

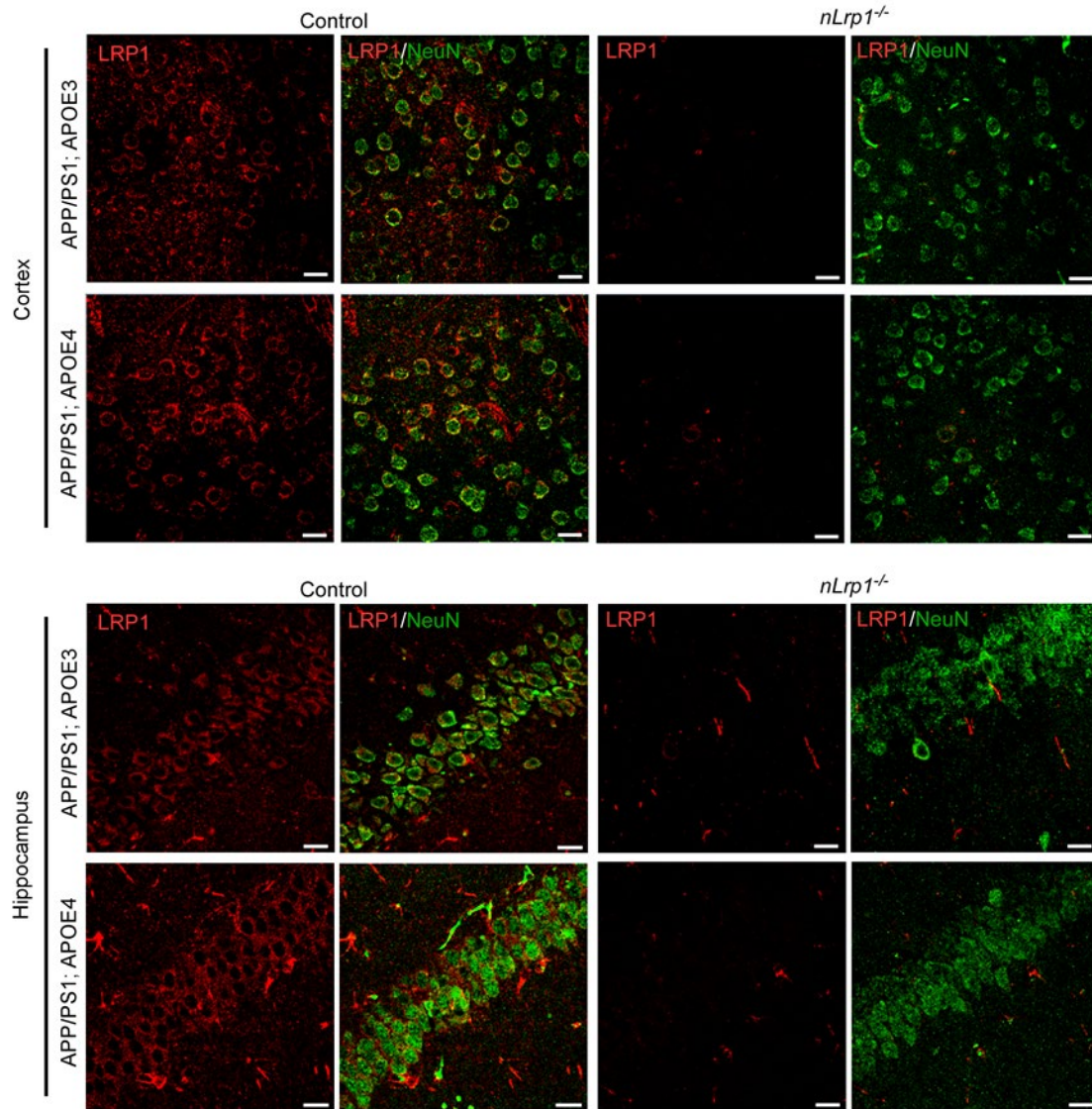
ELISA	Antibodies	Vendor	Catalog number
A β 40	Mouse monoclonal anti-human A β x-40 (13.1.1) capture antibody	In-house	(12, 13)
	Mouse monoclonal anti-human A β 1-16 (Ab5) detector antibody, HRP conjugated	In-house	(12, 13)
A β 42	Mouse monoclonal anti-human A β x-42 (2.1.3) capture antibody	In-house	(12, 13)
	Mouse monoclonal anti-human A β 1-16 (Ab5) detector antibody, HRP conjugated	In-house	(12, 13)
LRP1	Mouse monoclonal anti-LRP1 (6F8) capture antibody	Millipore	Cat# MABN1796
	Biotin-mouse monoclonal anti-LRP1 (5A6) detector antibody	Molecular Innovations	Cat# MA-5A6-BIO
LDLR	Rabbit polyclonal anti-LDLR (Irene) capture antibody	In-house	(12, 13)
	Biotin-goat polyclonal anti-human LDLR detector antibody	R&D Systems	Cat# BAF2148
ApoE	Goat polyclonal anti-apoE capture antibody	Millipore	Cat# AB947
	Biotin-goat polyclonal anti-apoE detector antibody	Meridian Life Science	Cat# K74180B
CTF β	Rabbit anti-C-terminus of APP capture antibody	In-house	(12, 13)
	Biotin-mouse monoclonal anti-human A β (N) (82E1) detector antibody	IBL-America	Cat#10326
GFAP	Rabbit polyclonal anti-GFAP capture antibody	US Biological	Cat# G2032-27J
	Mouse monoclonal anti-GFAP (GA5) detector antibody, biotin conjugated	Abcam	Cat# ab212398
CD11b	Rat monoclonal anti-CD11b/Integrin α M (M1/70) capture antibody	R&D Systems	Cat# MAB1124
	Rat monoclonal anti-CD11b (5C6) detector antibody, biotin conjugated	Bio-Rad	Cat# MCA711
PSD95	Rabbit polyclonal anti-PSD95 capture antibody	Osenses	Cat# OSD00037W
	Mouse monoclonal anti-PSD95 (K28/43) detector antibody, biotin conjugated	NeuroMab	Cat#75-028
Synapto-physin	Rabbit polyclonal anti-synaptophysin capture antibody	Osenses	Cat# OSS00021W
	Mouse monoclonal anti-synaptophysin (SY38) detector antibody, biotin conjugated	Origene	Cat# BM5519P



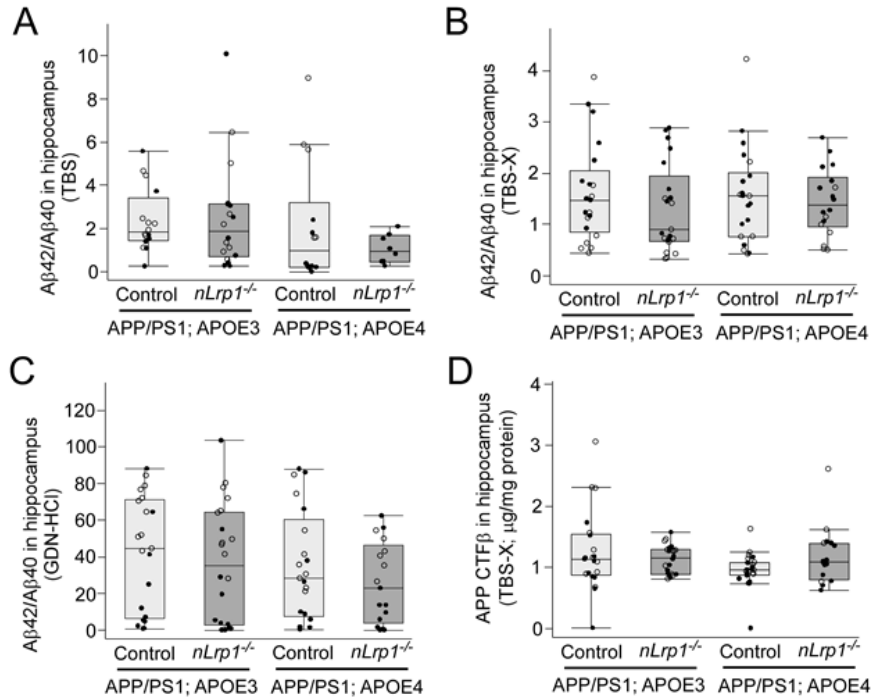
Supplemental figure 1. Effect of *APOE4* on the association between levels of LRP1 and soluble Aβ in AD brains. A-D, The concentrations of Aβ40 (A) and Aβ42 (B) in TBS fraction, and Aβ40 (C) and Aβ42 (D) in TBS-X fraction of the temporal cortex samples were plotted as they relate to *APOE* genotype. Horizontal lines, boxes, and whiskers correspond to median, interquartile range (IQR), and the furthest points within 1.5× IQR from the box, respectively (N=17-25/group). E-H, The regression plots for concentrations between LRP1-TBS Aβ40 (E), LRP1-TBS Aβ42 (F), LRP1-TBS-X Aβ40 (G), and LRP1-TBS-X Aβ42 (H) were presented. Their interactions were assessed by Analysis of Covariance by adjusting for age, sex, Braak stage, Thal and averaged CAA scores. R squares in each *APOE* genotype were as follow; (E) ε3/ε3, R²=0.0003, p=0.9465; ε3/ε4, R²=0.0477, p=0.3997; ε4/ε4, R²=0.0369, p=0.3579, (F) ε3/ε3, R²=0.3836, p=0.0061; ε3/ε4, R²=0.2494, p=0.0412; ε4/ε4, R²=0.0028, p=0.8022, (G) ε3/ε3, R²=0.0392, p=0.4309; ε3/ε4, R²=0.0843, p=0.2752; ε4/ε4, R²=0.0777, p=0.1733, and (H) ε3/ε3, R²=0.0113, p=0.6746; ε3/ε4, R²=0.3151, p=0.0191; ε4/ε4, R²=0.0104, p=0.6350. Open circles indicate data from females; closed circles indicate data from males.



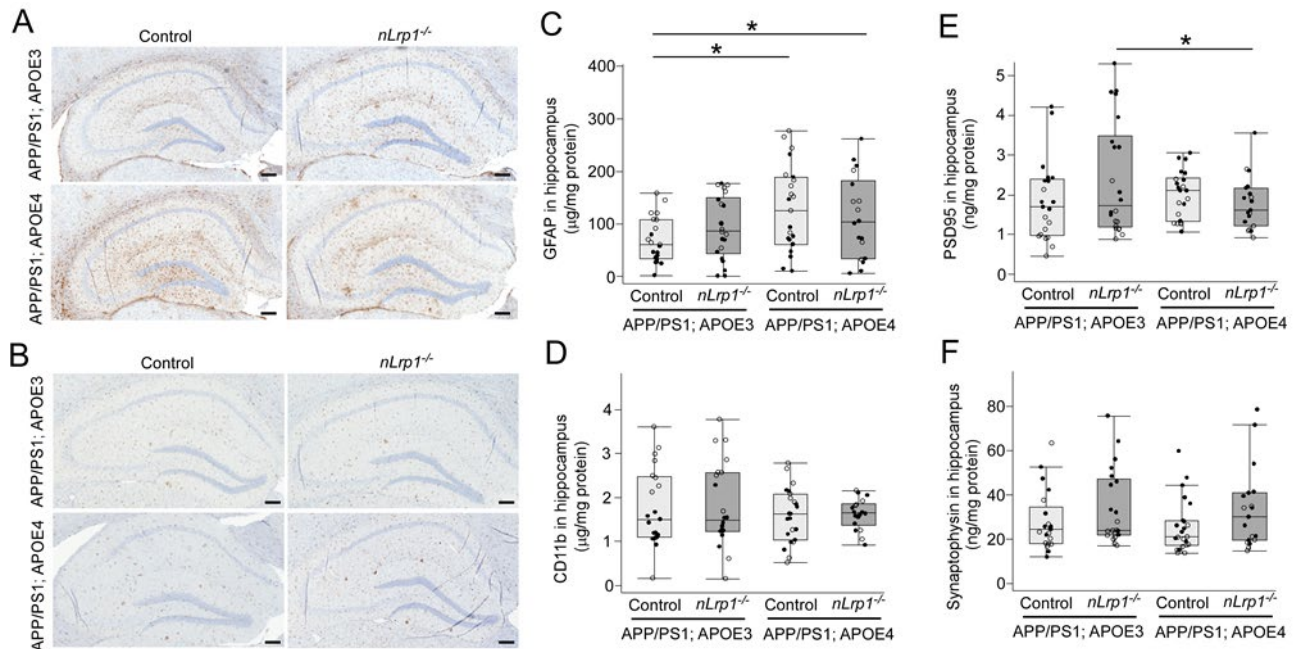
Supplemental figure 2. Effect of *APOE4* on the association between levels of LRP1 and CAA severity in AD brains. A, Averaged CAA scores were plotted as they relate to *APOE* genotype. Horizontal lines, boxes, and whiskers correspond to median, interquartile range (IQR), and the furthest points within $1.5 \times \text{IQR}$ from the box, respectively (N=17-25/group). B, The regression plot for LRP1 concentration and averaged CAA score are presented. Their interaction was assessed by Analysis of Covariance by adjusting for age, sex, Braak stage, and Thal score. R squares in each *APOE* genotype was as follow; $\epsilon 3/\epsilon 3$, $R^2=0.1588$, $p=0.1014$; $\epsilon 3/\epsilon 4$, $R^2=0.0036$, $p=0.8191$; $\epsilon 4/\epsilon 4$, $R^2=0.0338$, $p=0.3789$. Open circles indicate data from females; closed circles indicate data from males.



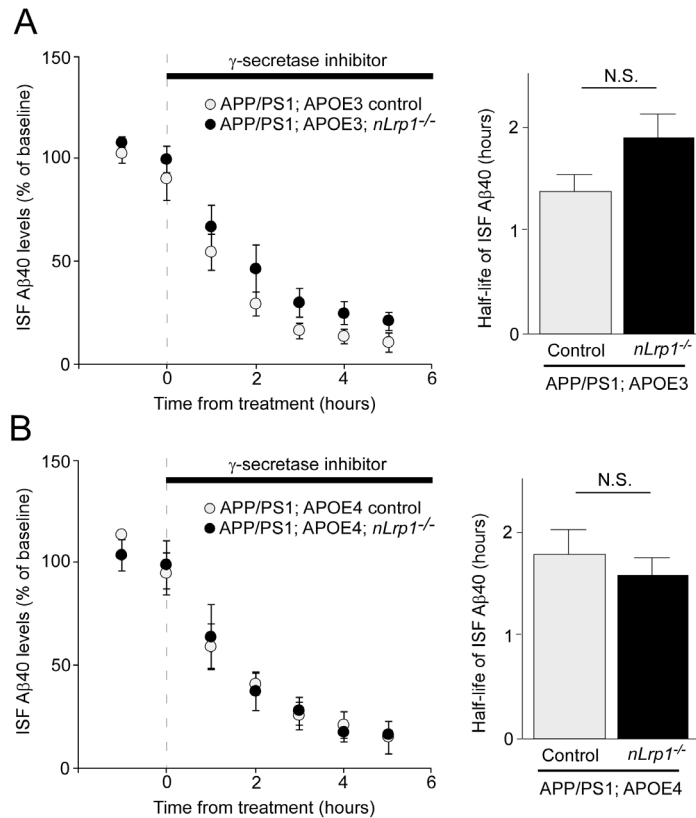
Supplemental figure 3. Immunostaining for LRP1 in the brains from APP/PS1; *nLrp1*^{-/-} with apoE3 or apoE4. Brain sections from APP/PS1; APOE3 control, APP/PS1; APOE3; *nLrp1*^{-/-}, APP/PS1; APOE4 control and APP/PS1; APOE4; *nLrp1*^{-/-} mice at the age of 9 months were stained for LRP1 (red) and a neuronal marker NeuN (green). Scale bar: 20 μ m.



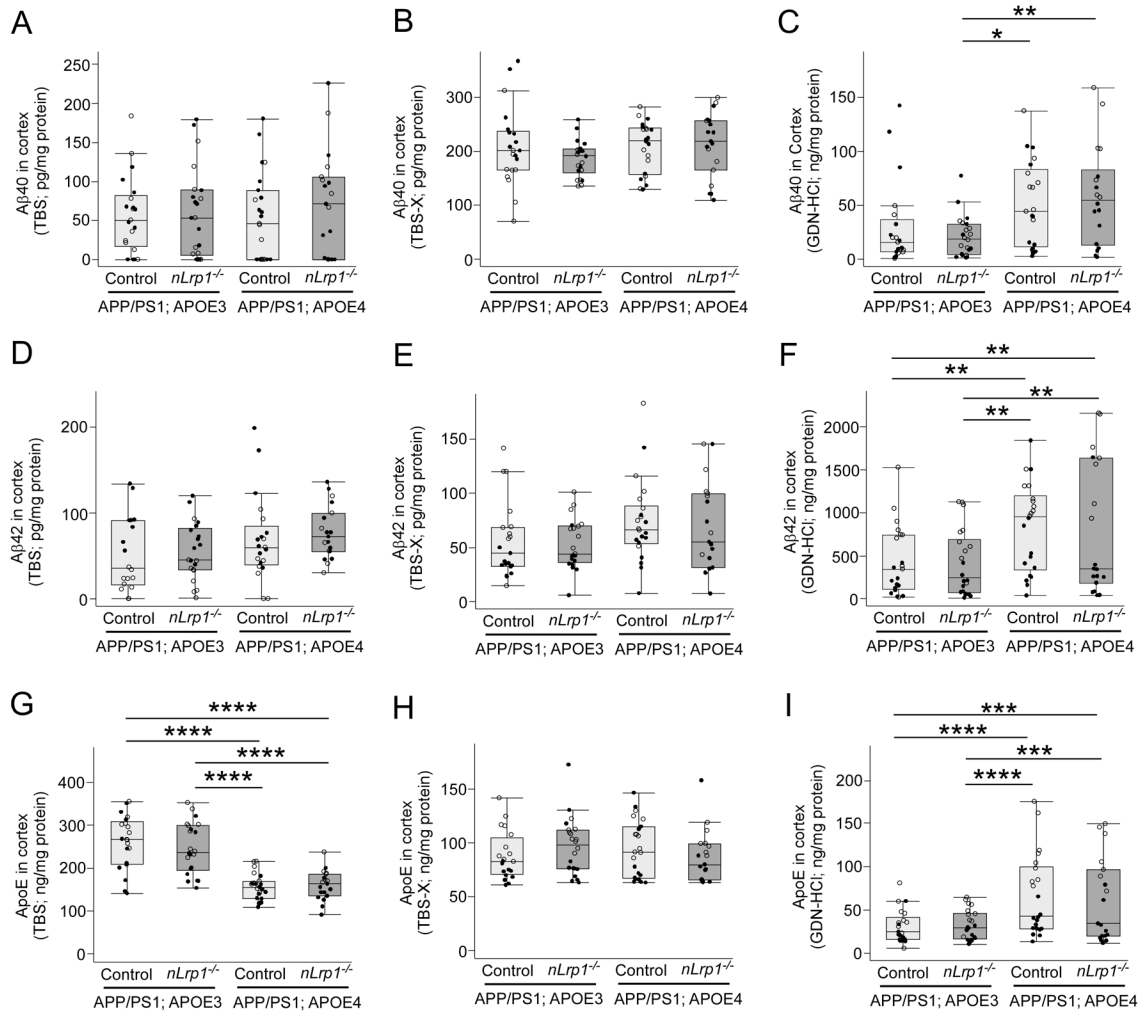
Supplemental figure 4. Neuronal LRP1 deficiency and apoE4 do not affect Aβ42/Aβ40 ratio or CTFβ levels in the hippocampus of APP/PS1 mice. The Aβ40/Aβ42 ratio in the hippocampus extracted in TBS (A), TBS-X (B) and GDN-HCl (C) fractions and CTFβ levels in TBS-X fraction (D) from APP/PS1; APOE3 control, APP/PS1; APOE3; *nLrp1*^{-/-}, APP/PS1; APOE4 control and APP/PS1; APOE4; *nLrp1*^{-/-} mice at 9 months old were plotted (N=16-23/group). Open and closed circles indicate data from female and male mice, respectively. Horizontal lines, boxes and whiskers correspond to medians, interquartile ranges (IQRs) and the furthest points within 1.5 x IQR from the box, respectively. Not significant by Tukey-Kramer's post-hoc analysis of two-way ANOVA.



Supplemental figure 5. Effects of neuronal LRP1 deficiency and apoE4 on glial activation and synaptic proteins in the hippocampus of APP/PS1 mice. Hippocampus from APP/PS1; APOE3 control, APP/PS1; APOE3; *nLrp1^{-/-}*, APP/PS1; APOE4 control and APP/PS1; APOE4; *nLrp1^{-/-}* mice were immunostained for GFAP (A) and Iba-1 (B) at 9 months old. Scale bar: 200 μm. The hippocampal amounts of GFAP (C), CD11b (D), PSD95 (E) and synaptophysin (F) in these mice were also measured by ELISA at 9 months of age (N=18-23/group). Open and closed circles indicate data from female and male mice, respectively. Horizontal lines, boxes and whiskers correspond to medians, interquartile ranges (IQRs) and the furthest points within 1.5 x IQR from the box, respectively. *, $p < 0.05$ by Tukey-Kramer's post-hoc analysis of two-way ANOVA.



Supplemental figure 6. Effects of apoE4 and neuronal LRP1 deficiency on A β clearance in the hippocampus of APP/PS1 mice. ISF A β 40 clearance was assessed using in vivo microdialysis in APP/PS1; APOE3 control, APP/PS1; APOE3; *nLrp1*^{-/-}, APP/PS1; APOE4 control and APP/PS1; APOE4; *nLrp1*^{-/-} mice at the age of 12-14 months (N=3-4 per group). The % baseline ISF A β 40 concentrations versus time were plotted for APP/PS1; APOE3 (A) and APP/PS1; APOE4 (B) mice. The slope from the individual linear regressions from log [% ISF-A β 40] versus time for each mouse was used to calculate the mean half-life ($t_{1/2}$) of elimination for A β 40 from the ISF. Values are mean \pm SEM. N.S., not significant two-tailed student's t test.



Supplemental figure 7. Effects of apoE4 and neuronal LRP1 deficiency on Aβ and apoE levels in the cortex of APP/PS1 mice. The concentrations of Aβ40 (A-C), Aβ42 (D-F) and apoE (G-I) in the cortex extracted in TBS, TBS-X and GDN-HCl from APP/PS1; APOE3 control, APP/PS1; APOE3; *nLrp1*^{-/-}, APP/PS1; APOE4 control and APP/PS1; APOE4; *nLrp1*^{-/-} mice were measured by ELISA at the age of 9 months (N=19-23/group). Open and closed circles indicate data from female and male mice, respectively. Horizontal lines, boxes and whiskers correspond to medians, interquartile ranges (IQRs) and the furthest points within 1.5 x IQR from the box, respectively. *, p < 0.05; **, p < 0.01; ***, p < 0.001; ****, p < 0.0001 by Tukey-Kramer's post-hoc analysis of two-way ANOVA.